Journal of Photochemistry & Photobiology A: Chemistry 367 (2018) 411–419

Contents lists available at ScienceDirect

Journal of Photochemistry & Photobiology A: Chemistry

journal homepage: www.elsevier.com/locate/jphotochem

Ultrafast transient absorption spectra of photoexcited YOYO-1 molecules call for additional investigations of their fluorescence quenching mechanism

Lei Wang[1], Joseph R. Pyle[1], Katherine L.A. Cimatu*, Jixin Chen*

Ohio University, Department of Chemistry and Biochemistry, Athens, OH, 45701, USA

ARTICLE INFO

Keywords:
Transient absorption spectroscopy
Intermolecular charge transfer
Photochemical kinetics
Fluorescence quenching

ABSTRACT

In this report, we observed that YOYO-1 immobilized on a glass surface is much brighter when dried (quantum yield 16 ± 4% in the ambient air) or in hexane than in water (quantum yield ~0%). YOYO-1 is a typical cyanine dye that has a photo-isomerization reaction upon light illumination. In order to understand this quenching mechanism, we use femtosecond transient absorption spectroscopy to measure YOYO-1's electron dynamics after excitation directly. By deconvoluting the hot-ground-state absorption and the stimulated emission, the dynamics of electronic relaxation and balance are revealed. The results support the intermolecular charge transfer mechanism better than the intramolecular relaxation mechanism that has been widely believed before. We believe that the first step of the relaxation involves a Dexter charge transfer between the photo-excited YOYO-1 molecule and another guest molecule that is directly bound to the YOYO-1 giving two radicals with opposite signs of charges. The charges are recombined either directly between these two molecules, or both molecules start to rotate and separate from each other. Eventually, the two charges recombined non-radiatively via various pathways. These pathways are reflected on the complicated multi-exponential decay curves of YOYO-1 fluorescence lifetime measurements. This charge transfer mechanism suggests that (1) electrical insulation may help improve the quantum yield of YOYO-1 in polar solutions significantly and (2) a steric hindrance for the intramolecular rotation may have a less significant effect.

1. Introduction

The fluorescence quenching mechanisms of a typical organic dye have been summarized in the literature to be a vibrational or/and electrical relaxation of the excited electrons through major pathways shown in Fig. 1, namely, intramolecular relaxation, and intermolecular/intermoiety relaxation including energy transfer (e.g. Förster resonance energy transfer, FRET) and charge separation pathways [1]. Among these, photo-induced charge separation (via electron or hydrogen transfer) is one of the most fundamental processes in chemistry and biology that has been extensively investigated by diverse experimental and theoretical methods [2–12]. For example, ultrafast charge transfer (100 fs) from solvents to Nile Blue A perchlorate (NB) has been reported by Yashihara et al. to be responsible for NB's fluorescent quenching [10], and the same mechanism has been used to explain the fluorescence quenching of oxazines and coumarines [8,13–15].

Here we report a study on the fluorescent quenching mechanism of a typical cyanine dye, YOYO-1 (Fig. 2A), for which intramolecular charge transfer has been considered the major mechanism [16–20]. YOYO-1, an oxazole yellow (YO) dimer and a member of the YOYO-TOTO family of cyanine dyes belonging to the polymethine group, is a widely used DNA fluorescent staining dye [21–23]. YOYO-1 has a high photon molar absorptivity, with peak extinction coefficient at a visible wavelength approaching $10^5\,cm^{-1}M^{-1}$ [22]. The fluorescence quantum yield of YOYO-1 in water is usually very small (< 0.1%) and thus is nonfluorescent. Upon binding to DNA, its quantum yield enhances over 1000 fold and reaches up to 50% [22,24]. This huge fluorescence contrast has caused a revolution in molecular biology in the 1990s [25], which enabled visualization and detection of DNA molecules using fluorescent molecules instead of radioactive molecules. The quenching mechanism of the YOYO-1 fluorescence in water has been attributed to the nonradiative decay of excited electrons via the rotation/torsion of the benzoxazole and quinolinium moieties at the methine bridge (photo-isomerization) [17], a mechanism proposed for typical polymethine dyes [19,26,27,28,29,30]. Theoretical calculations have suggested that the initial rotation is induced by an intramolecular twisted internal charge transfer (TICT) [19]. In this report, we use

* Corresponding authors.
E-mail addresses: cimatu@ohio.edu (K.L.A. Cimatu), chenj@ohio.edu (J. Chen).
[1] Both authors contribute equally.

https://doi.org/10.1016/j.jphotochem.2018.09.012
Received 3 July 2018; Received in revised form 22 August 2018; Accepted 8 September 2018
Available online 10 September 2018
1010-6030/

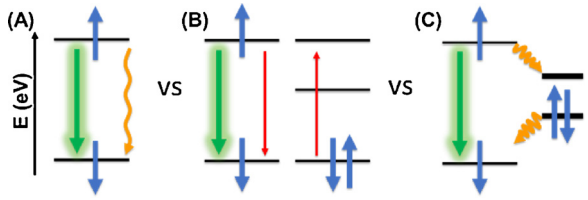

Fig. 1. Scheme of simplified fluorescence quenching mechanisms, self-quenched (intramolecular) or quenched by other molecules (intermolecular) [1]. (A) An electron energy diagram of fluorescent and vibrational relaxation of an excited molecule. Blue arrows are electrons with spin, each black line is an electronic orbital, green arrows are fluorescent emission, and orange arrows are thermal relaxation. (B) Energy transfer where the red arrows indicate the energy exchange between two molecules. (C) Charge transfer to another molecule that is directly connected to the molecule.

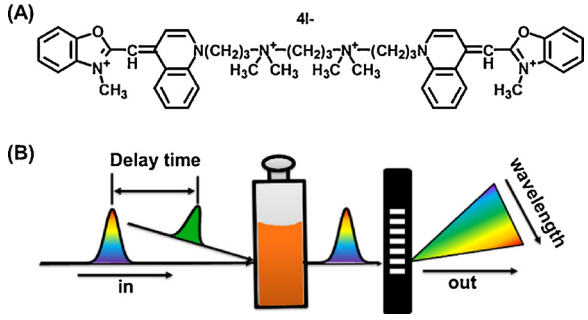

Fig. 2. (A) Chemical structure of YOYO-1. (B) Scheme of time-resolved transient absorption spectroscopy. Pump (green) and probe (rainbow) lasers pass through a sample with a delay time between them, and then the probe pulse is analyzed with a spectrometer. The TA signal is the difference in absorbance of the probe before and after excitation.

femtosecond time-resolved transient absorption (**TA**) spectroscopy (Fig. 2B) that has been widely used for photo-induced electron dynamics [18,31–36], to revisit YOYO-1's quenching mechanism. We are particularly comparing the intramolecular TICT relaxation and the intermolecular charge-transfer mechanism.

2. Experimental section

2.1. Fluorescent imaging of YOYO-1

It was carried out with a 473 nm solid-state excitation laser (Dragon Lasers, China) either under total internal reflection fluorescence (TIRF) or epifluorescence (EPI) mode; Nikon Ti-U inverted microscope with a Nikon 100× oil-immersed TIRF objective (CFI Apo 100×, NA 1.49, WD 0.12 mm); a fluorescent filter cube with ZET488/10 laser bandpass filter, ZT488rdc dichroic mirror, and ET500lp long pass filter (Chroma, USA); and an EMCCD camera (Andor iXon Ultra 897, USA) [21].

Glass coverslips and tweezers were cleaned by first sonicating in soap (Liquinox) water and secondly using "base piranha" solution (*caution* for corrosive and splashing). The glass coverslips were washed with ultrapure water after each step and were stored in ultrapure water before use. All cleaned glass coverslips used in these experiments were confirmed to have no fluorescent contamination at the single-molecule level by measuring them before experiments (*i.e.* no fluorescent spot was observed when searching around the nitrogen blown dry glass coverslips). A volume of 10 µL of the solvents, ultrapure water, ethanol (200 proof, Sigma-Aldrich), and hexane (GC grade > 99.9%, B&J Brand), were dropped on the clean glasses, dried, and measured. No detectable single-molecule fluorescent signals were observed.

YOYO-1 parent solution (0.1 mM in water) was diluted in ultrapure water to make 0.1 µM, 0.1 nM, and 1 pM solutions. Rhodamine 6 G (99%, Sigma-Aldrich) was dissolved in ethanol and its absorbance was measured to be 0.763 at 530 nm (extinction coefficient 116,000 cm^{-1}/M) that corresponds to the concentration of 6.6 µM. This solution was used to make a 1 pM solution.

The high-coverage YOYO-1/glass sample was made by dropping YOYO-1 aqueous solution (0.1 µM, 10 µL) on a glass coverslip and incubated for about 30 s before it was rinsed away by water for about 30 s and blown dry with nitrogen. This sample was imaged during which water and hexane were dropped on and dried alternately (room humidity 17%) both at TIRF and EPI mode. Excitation laser power density was tuned to 18 W/cm^2, camera electron-multiplying (EM) gain was set to 50, and the exposure time was 0.02 s per picture. The low-coverage YOYO-1/glass sample was prepared by dropping YOYO-1 solution (1 pM, 3 µL) on a glass coverslip and dried. Low-coverage rhodamine 6 G/glass sample was prepared by dropping rhodamine 6 G solution (1 pM, 3 µL) on a glass coverslip and dried. Laser power density was tuned to 12 W/cm^2, camera EM gain was set to 300, and the exposure time was 0.05 s for single-molecule fluorescence measurements. The histograms of single-molecule intensity were obtained by selecting molecules whose intensities were > 5 times the noise level of the fluorescent image.

2.2. UV–vis spectra

They were collected with an Ocean Optics USB2000 spectrometer and an Agilent 8453 spectrometer. UV–vis and steady-state fluorescent spectra were fitted using software Fityk (free version) with Voigt functions.

2.3. Femtosecond transient absorption spectroscopy

Three solutions for TA measurements were prepared using reagents without further purifications. The water used in sample preparation was an ultrapure deionized (DI) water (18.2 MΩ cm from Barnstead E-pure system). YOYO-1 in dimethyl sulfoxide (DMSO) (Invitrogen, Thermo Fisher Scientific) was diluted to 10 µM in ultrapure water, or DMSO (Sigma-Aldrich) for the two solutions of YOYO-1/water and YOYO-1/DMSO, respectively. This relative low concentration is chosen to avoid the formation of H-aggregation or J-aggregation of YOYO-1 in the solutions. YOYO-1/DNA solution (300 µg/mL) was made by adding phage Lambda DNA (48,502 basepairs, Thermo Fisher Scientific) to the buffer solution of 25 mM HEPES (pH 7.4, Sigma-Aldrich), 20 mM NaCl (Sigma-Aldrich), and 2 mM $MgCl_2$ (Ambion, Thermo Fisher Scientific). The YOYO-1 to DNA basepair ratio was calculated to be 1:46 assuming an average molecular weight per basepair of 650 daltons for double-stranded DNA with sodium salt. The relatively small dye-DNA ratio minimizes the concentration of free and non-intercalated YOYO-1. The solutions were heated to 40 °C and vacuumed two minutes to remove air bubbles, and the DNA samples were incubated overnight before the TA measurements.

Femtosecond TA spectra were collected on a HELIOS femtosecond transient absorption spectrometer (Ultrafast Systems, USA). The instrumental setup and the experimental procedures were reported previously [31,37,38]. The pump laser was set to 486 ± 1 nm whose power was adjusted to 185 ± 5 µW, and the probe white-light laser was measured at 30 ± 5 µW. Under these conditions, nonlinear laser effects or two-photon absorption, and photobleaching were negligible or minimal. The repetition rate was 1 kHz, and the pump-probe pulse convoluted width was ~150 fs. During the experiments, the sample solutions were irradiated with an absorbance of 0.2 measured at the excitation wavelength in a 2.0 mm path length cuvette under mild stirring. All TA data were corrected by subtracting spectral background features that persisted from the previous pulse and appeared pre-pulse, as well as applying chirp and t_0 corrections.

A home-written MATLAB code was used to analyze the TA spectral data which was represented from the Surface Xplorer Pro 1.1.5 software that came with the instrument (see its online manual for details) [39].

The spectra were further analysed with 2D correlation method reported in the literature by Noda [40]. The time traces were fitted with a multi-exponential function ($y_{fit} = \sum A_i e^{-t/\tau_i}$) that was convoluted with the instrument response function (IRF) using MATLAB. The standard deviations were obtained by fitting different measurements using the same set of initial guesses [41].

2.4. DFT calculations

They were carried out in Gaussian 09 D.01 [42] using B3LYP [42] hybrid functional with 6-311G+(d,p) [43] basis sets. Single-molecule fluorescent data were analysed using the open-source MATLAB codes reported before [21,44–46].

3. Results

To compare the mechanisms shown in Fig. 1 and re-evaluate the significant ones, we measure the fluorescent signal of YOYO-1 in polar and non-polar solvents. Because YOYO-1 is insoluble in non-polar solvents, bulk solution measurements are difficult. We adsorb the YOYO-1 onto a glass surface so that we can change solvents freely. Before data collection, we confirmed that the cleaned glass and all solvents do not have any fluorescent contamination under the 473 nm laser excitation. Dried YOYO-1 on the glass results in a bright image compared to the scratches where the dye is removed by a tweezer tip (Fig. 3A). It becomes extremely weak with a water-drop on it which is consistent with the bulk solution measurements that the fluorescence quantum yield of YOYO-1 in water is almost zero. A small number of molecules may have been washed away but a photobleaching test left a clear bleaching mark on the dried sample, which confirms that the majority dyes stay. When dropping hexane (non-polar) on the glass surface, the fluorescence intensity drops to about half of that in the air (Fig. 3B). These measurements are repeated by dropping and drying alternately to confirm reproducibility. The measurements are done both on TIRF and EPI modes obtaining similar results suggesting that intensity change is not because of excitation variation. At the single-molecule level, dried YOYO-1 is also bright (Fig. 3C). Its intensity is compared to single-molecule rhodamine 6 G (R6 G) (Fig. 3D). These bright spots are confirmed to be the molecule of interest by dropping more solutions and dried to confirm the increase of coverage upon addition, and the solvents have been confirmed to be clean. The coverage is consistent with the calculated coverage of 3 μL of a 1 pM solution covering a ~1 cm^2 area, which gives a surface coverage 1.8×10^{10} m^{-2}, or ~20 molecules per area in Fig. 3**C** and **D**. We see bright YOYO-1 when we drop hexane on the glass. We don't observe single-molecule YOYO-1 in water.

The quantitative quantum-yield analysis is carried out only for the dried samples using a single-molecule method established in the literature [47]. Dried single-molecule samples avoid the bias from possible variations of the excitation intensities, aggregation, and washing on the high molecular coverage samples. Using the standard R6 G dye as a reference, the fluorescence quantum yield of dried YOYO-1 is calculated 16 ± 4% (See the next paragraph for the calculations), which is > 500 times the quantum yield of YOYO-1 in water (almost three orders of magnitude increase) and is comparable to (~1/3) the quantum yield of those intercalated in a DNA molecule. The experiment has been carried out under ambient conditions with 17% relative humidity. Removing water and oxygen in the air may further increase the quantum yield value.

Under the same conditions for the instrumentation set-up, the average fitted maximum of the point spread function of single-molecule YOYO-1 is 2500 ± 900 photocounts and R6 G is 2600 ± 500 photocounts, respectively (Fig. 3E). The extinction coefficient of R6 G at 473 nm is 1.1×10^4 $cm^{-1}M^{-1}$, and its fluorescence quantum yield is > 95% [48]. The extinction coefficient of YOYO-1 at 473 nm is 7.3×10^4 cm^{-1} M^{-1} [24]. Our long-pass filter cuts 11% YOYO-1 emission signal and allows all R6 G signal to pass. The EMCCD detector has a uniform sensitivity on both the YOYO-1 and the R6 G emissions wavelengths. Assuming a small molecular orientational effect because the excitation and collection angle of our 100× objective spans most of the whole half sphere (−77° to 77°, with objective NA 1.49, and the refractive index 1.53 for both glass and the objective immersion oil), the quantum yield of dried YOYO-1 on glass can be calculated using the Beer–Lambert law and referenced to the R6 G standard. The extinction coefficient of the dye is measured using solution transmission:

$$A = \log_{10}\frac{I_0}{I_T} = lc\varepsilon \quad (1)$$

where A is the absorbance, I_0 is the incident photon flux, I_T is the transmitted photon flux, l is the optical path length of the solution, c is the concentration of the dye in the solution, and ε is its extinction coefficient. Thus for a 1 μM solution in a 1 cm long cuvette when the precondition is met, i.e. each photon passes less than one molecule, the absorbance of YOYO-1 is 1.18 and R6 G is 1.03 at 473 nm, meaning that each YOYO-1 molecule absorbs $(7.3 \times 10^4)/(1.1 \times 10^4) = 6.6$ times more photons than each R6 G molecule at this wavelength, i.e., a YOYO-1 molecule has 6.6 times larger absorption cross section than an

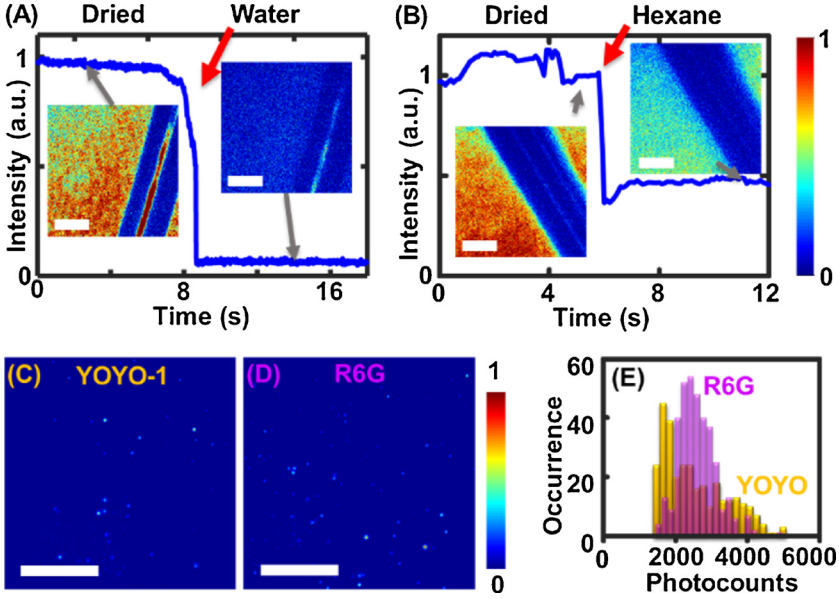

Fig. 3. Normalized average photocounts of YOYO-1/glass (high coverage) (A) before and after dropping pure water indicated by the red arrows, and (B) pure hexane on the glass coverslip. Insets and the grey arrows show example fluorescent images that have the same color scale representing intensities. The dark scratches are created by a tweezer tip. Relatively large intensity fluctuations in (A and B) are caused by the moving pipette tip. Fluorescent images of single-molecule (C) YOYO-1, and (D) rhodamine 6 G dried on clean glass coverslips. (E) Histograms of the bright spots (intensities > 5 times the standard deviation of the image noise) on the fluorescent images (magenta is the overlap part). All scale bars are 10 μm.

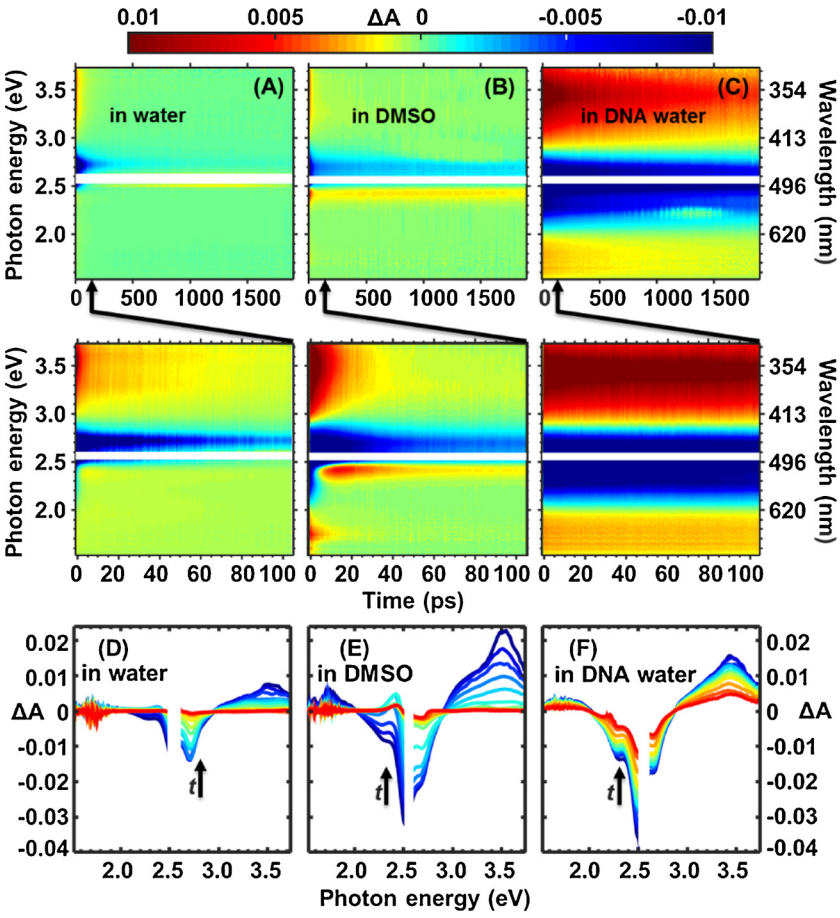

Fig. 4. The probe TA spectra change (Δ*A*) after the pump excitation of 10 μM YOYO-1 (A) in water, (B) in DMSO, and (C) 460 μM DNA basepair (300 μg/mL phage λ-DNA) upon different pump-probe delay times. The lower row is the zoom-in of the first 100 ps in the spectra above. Experiments were repeated with two sets of different samples on different days. Consistency has been observed. Pump pulse is 100 fs, 486 nm (2.55 eV) laser; and probe pulse is 100 fs, white light laser. (D–F) Sample spectra in (A–C) over delay time 0.5, 1, 2, 5, 10, 20, 50, 100, 200, 500, 1000, and 1500 ps.

R6 G molecule at 473 nm.

Fluorescence quantum yield of a molecule is defined as the number of emitted photons of interest over the number of absorbed photons. Thus, the average quantum yield of these bright YOYO-1 molecules is

$$QY = QY_R \frac{Em/D}{\left(\frac{\varepsilon}{\varepsilon_R}\right) Em_R/D_R} \quad (2)$$

where QY_R is the quantum yield of the reference molecule, *E*m is the detected average emission, and D/D_R is the relative photon collection efficiency between the molecule and the reference. Thus, dried YOYO-1 QY = 95% × (2500/89%)/6.6/(2600/100%) = 16 ± 4%. The error bar is estimated from the distribution of the emission intensities.

TA has been demonstrated as a powerful technique in measuring charge transfer [18] [33–36], thus we measured the TA spectra of YOYO-1 molecules in three different solutions, namely in water, DMSO, and a DNA buffer solution (Fig. 4). YOYO-1 only dissolves in polar solvents. Thus, we cannot measure YOYO-1 TA in non-polar solvents. When intercalated into DNA basepairs, the two head groups of YOYO-1 are in a hydrophobic environment and the linker part of YOYO-1 is at the water-DNA interface. The dynamics of the excited electron decay is observed in the positive (red) parts of the TA spectra in Fig. 4. A low dye concentration (10^{-5} M) is selected to minimize the intermolecular aggregation of dyes in the solution. The depleted-ground-state refill is observed in most of the negative (blue) parts of Fig. 4. The absorbance signal after the pulsed laser excitation has been referenced to the absorbance of the solution before the excitation. Thus, a positive signal indicates the concentration increase of the species it represents after excitation than before excitation and a negative signal indicates a concentration decrease. The steady-state UV–vis spectra and fluorescent emission spectra of YOYO-1 are available in the supporting information as **Figs. S1-S3**. The relationship between the different TA absorption peaks is shown in the supporting information **Fig. S4** via the 2D-correlation analysis [40,49–52], on which a positive correlation means that the two signals go up and down over time synchronously, and a negative value means an anti-correlation.

The peaks in the TA spectra are assigned (Fig. 5) based on YOYO-1's UV–vis absorption spectra (supporting information **Figs. S1, S2**), fluorescence emission spectra (supporting information **Fig. S3**), and 2D correlation spectra of the TA measurements (supporting information **Fig. S4**). First, from the UV–vis absorption spectra, three bands of absorption are observed for YOYO-1, with absorption energy centered around 2.5 eV (496 nm), 4 eV (310 nm), and > 5 eV (248 nm), respectively (supporting information **Fig. S2**). These three bands represent the energy gaps between the ground state (S_0) and three separated groups of excited states named S_1, S_2, and S_3 respectively. The S_0-S_3 absorption overlaps with the quartz cuvette absorption range (starts above ~7 eV and goes up) thus its energy center cannot be determined from the spectra. Second, the fluorescent emission is Stokes shifted from the S_0-S_1 absorption of about 0.2 eV (~40 nm) (supporting information **Fig. S3**). Usually, the fluorescence has randomly-oriented emission angles during a regular fluorescent experiment and would be undetectable for a detector positioned relatively far away. However, in the TA experiment, the probe stimulates the emission in the same direction, with the emission intensity as a function of the probe intensity, spectral overlap, and the population of the excited-state molecules [53]. Thus, stimulated emission (**SE**) is often observed in TA experiments [32]. The dynamics of the transient absorption bands also help in the peak assignments because the bands originating from the same excited electrons will have the same or similar decay dynamics and will show positive correlations among them on the 2D correlation spectra (supporting information **Fig. S4**).

The band with two peaks at 2.54 eV and 2.71 eV is apparently the

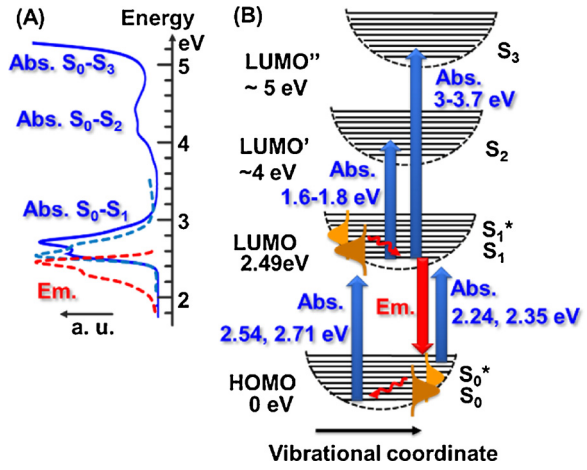

Fig. 5. (A) YOYO-1 absorption and emission spectra in energy scale. The blue solid line is the absorption of YOYO-1 in water, the blue dashed line is the YOYO-1 absorption in DNA, and the red dashed line is the YOYO-1 emission in DNA. (B) Scheme of band assignment in the TA spectra. The YOYO-1 molecular orbitals are coupled with its atomic nucleus vibrations (Franck-Condon principle) to represent a distribution of molecules with the same electronic structure but different vibrational states in the solution at a given moment. S_n indicates one excited electron on the n^{th} electronic orbital (often delocalized) and another electron in the ground state leaving a vacancy on the HOMO of the original host atom of the excited electron right after the excitation (delocalized over time). Arrows show the absorptions (blue arrows), the vibrational relaxation (twisted red arrows), and the emission (straight red arrow) of YOYO-1.

ground-state depletion after the excitation, because they have the same peak position values in the S_0-S_1 band of the steady-state UV–vis absorption spectra, which represents the energy gap between the highest occupied molecular orbital (HOMO) and the lowest unoccupied molecular orbital (LUMO). The initially negative TA signal of this band represents the decrease of the ground-state-molecule concentration in the solution after excitation, and its dynamics represents the rebuilding of the ground-state population that has been depleted by the pump laser. This band is negative for the three solutions and goes back to zero at very different rates. The 1.7 eV and 3.4 eV band is the excited state absorption of LUMO electrons (the same as calculated from the energy gaps in the steady-state absorption spectra) [32]. These two bands are positively correlated with each other and are negatively correlated with the ground-state repopulation, perfectly representing the LUMO (lose) to HOMO (gain) electron relaxation. These two bands are all positive at the beginning and decay back to zero in the three solutions. The steady-state S_0-S_3 band (> 5 eV) overlaps with the quartz absorption, but the S_1-S_3 transition in the TA spectra can be well resolved at about 3.4 eV (Figs. 4 and 5). The transitions of S_0-S_2 and S_0-S_3 are ~4 eV and 5.5 eV, respectively. These two bands are positioned beyond the energy window of our probe laser.

The band around 2.24 eV and 2.35 eV is the combination of the fluorescence stimulated emission (**SE**) [32], and the absorption of HOMO electrons when the molecules are at an upper vibrational level (S_0*) [54]. The SE peaks have the same energies on the steady-state fluorescent emission spectrum and S_0* is called the Franck-Condon ground state or the hot-ground-state [55–57]. At the same time, the molecule can undergo photoisomerization. These assignments are supported by the 2D correlation analysis (supporting information **Fig. S4**). The positive correlation between 1.7 eV and 3.4 eV (red color) groups them both as contributing from the excited LUMO electrons of the molecules at S_1 excited state, both being anti-correlated to the HOMO electron absorption (e.g., the band at 2.54 eV). Condition-dependent positive and negative correlation between 2.54 eV and 2.24 eV split the origin of 2.24 eV signal, coming from the excited electrons of molecules either at S_0* or at S_1 states competing with each other under different conditions. This assignment explains why the band is negative right after excitation in all three solutions. At this moment, the excited-state molecules have a large population which contributes to a large **SE** signal, and the hot-ground-state population is zero which does not contribute to any signal. As time goes by in the water, the relaxation of the excited molecule is very fast (a few ps), which relaxes mostly to the ground state such that the **SE** signal becomes very small. A small population of the excited-state molecules relaxes to the hot-ground-state (S_0*) and eventually relaxes back to the ground state. These hot-ground-state molecules contribute to a small positive signal at around 5 ps that vanishes back to zero later. In DMSO, the excitation state also relaxes fast (~20 ps), but a more substantial portion goes to the hot-ground-state. Thus, the signal dramatically overshoots to a relatively large positive value at ~10 ps (red color at 2.35 eV, 10 ps on Fig. 4B). This signal stays positive for a longer time and then relaxes in ~50 ps, with a small portion remaining positive even after 1 ns. In DNA, the excited-state population remains large and the hot-ground-state population is small throughout our experimental time window. Thus, only the negative signal is observed, because the **SE** signal dominates the S_0* absorption.

A target analysis strategy, which has been commonly used in the data analysis of time-resolved spectra [41], is used to analyze the decay curves of the TA spectra with a two-step electron transfer model shown

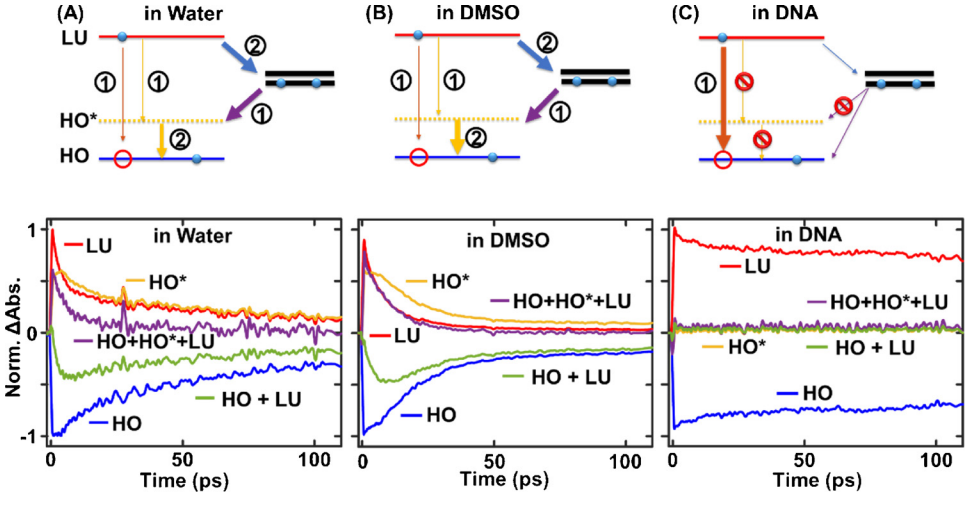

Fig. 6. Scheme of a two-step Dexter electron transfer mechanism (top) based on the normalized absorption decays (bottom) that represent the concentration of molecules with different electronic states vs pulse delay time for YOYO-1 in.(A) water, (B) DMSO, and (C) DNA solutions. (Top) Lines represent energy levels (molecular orbitals), blue dots represent electrons, red circles represent available space for electrons on the HOMO, black states represent unknown molecules that can donate and accept electrons, and arrows represent the electron decay pathways. The numbers in the scheme represent the order in the time series. (Bottom) Negative values in the decay curves mean the loss of electrons after excitation and positive values represent the excited electrons. The red curve (representing ^{1}|HO LU > absorbance) and blue curve (representing ^{1}|HO HO > absorbance) are normalized raw data, the green curve is the sum of these two, the orange curve (representing ^{1}|HO* HO* > absorbance) is calculated from two curves explained in the main text, and the purple curve is the sum of the orange and green curves.

in Fig. 6. Within this model, right after the pump laser excitation, YOYO-1 has ground-state depletion (some molecules are excited), leaving an electron vacancy at HOMO, and an excited electron at LUMO. Thus, the excited molecule stays electrically neutral with a possible (oscillating) dipole formation at $^1|$HO LU $>$. These electrons have intramolecular charge transfer nature according to theoretical calculations on the model system stilbene [19]. The energy structure of the excited molecules remains largely unchanged because no significant peak shifting is observed in the TA measurement and the excited electrons absorb light consistent with the gap of the ground-state absorptions (Fig. 5): 1.7 eV consistent with the gap between absorption peaks representing S_0-S_1 and S_0-S_2 transitions, and 3.4 eV consistent with the gap between absorption peaks representing S_0-S_1 and S_0-S_3 transitions. The electron vacancy at HOMO gives a negative ΔA in the TA spectra, and the LUMO electron gives a positive ΔA signal. At time zero, no charge transfer is expected such that the sum of these two signal is zero. The absorption cross section of the missing HOMO electron (hole) before excitation to a 2.71 eV light and the excited electron after excitation to a 3.44 eV light have similar magnitudes but opposite signs on the TA spectra (Fig. 4**D-E**). At time zero, their concentration should be the same. Thus, we normalize the 2.71 eV decay curve representing the electron vacancy concentration at HOMO (concentration of molecules with a missing electron in the HOMO) to -1 and normalize the 3.44 eV decay curve representing the electron concentration at LUMO (concentration of molecules with an excited electron in the LUMO) to 1 at time zero, such that the sum of both equals zero at time zero.

The asymmetry between the curves of electron vacancy in HOMO and excited electrons in LUMO in water and DMSO suggests that a simplified picture of the relaxation pathway shown in Fig. 1**A** fails. If the only available pathways for the LUMO electrons to decay back to the HOMO are via fluorescence and thermal relaxation, the sum (the green curve HO + LU in Fig. 6) of the HOMO and the LUMO decay curves (the red and the blue curves in Fig. 6) would have remained at zero as a function of time, and a symmetric decay pattern would have been observed. However, when adding the two experimental decay curves of HOMO and LUMO, a negative signal is obtained in both water (Fig. 6**A** green curve) and DMSO (Fig. 6**B** green curve), while conservation is observed in the DNA solution (Fig. 6**C** green curve). At first, we have considered that all the missing electrons relax to the hot-ground-state HOMO* when both electrons are at the HOMO, but the nuclei are at higher vibrational levels. Thus, we further analyze the concentrations of molecules at S_0*.

The decay curve at 2.35 eV contains HOMO* electron absorption, and the fluorescence stimulated emission signal (negative signal) whose intensity is directly proportional to the concentration of molecules at S_1. Thus the absorbance of the electrons in HOMO* (Fig. 6 orange curves) can be deconvoluted from the decay curve at 2.35 eV ($A_{2.35eV}$) and the absorbance of the excited electrons (A_{LU}). The probe laser with intensity I_0 passes the sample and gives a new light intensity

$$I_0 \rightarrow sample \rightarrow (I_T + I_{SE})$$

where I_T is the transmitting light intensity, and I_{SE} is the fluorescence stimulated emission intensity. Thus, the measured TA signal at 2.35 eV is

$$A_{2.35eV} = \log_{10}\frac{I_0}{I_T + I_{SE}} \tag{3}$$

In which the absorbance of the molecules at hot-ground-state is

$$A_{HO^*} = \log_{10}\frac{I_0}{I_T} \tag{4}$$

and the stimulated emission intensity I_{SE} is proportional to the concentration of the LUMO electrons and eventually the absorbance of the LUMO electrons A_{LU}:

$$I_{SE} = aA_{LU} \tag{5}$$

where a is a constant.

Once we apply the boundary condition that at time = 0, A_{HO^*} (@ $t = 0$) = 0, and I_T (@ $t = 0$) = I_0 (no absorption, Eq. (4)) at 2.35 eV in Eqs. (3) and (5), we obtain

$$10^{A_{2.35eV}} = \frac{I_0}{I_0 + aA_{LU}}(@\, t = 0)\ thus$$

$$a = \frac{I_0}{10^{A2.35eV}A_{LU}} - \frac{I_0}{A_{LU}}(@\, t = 0)\ Let$$

$$a = kI_0,$$

where $k = \frac{1}{10^{A2.35eV}A_{LU}} - \frac{1}{A_{LU}}$ (@ t = 0) is a constant,

$A_{2.35eV}$ (@$t = 0$) is the measured TA value at 2.35 eV and time zero, A_{LU} (@$t = 0$) is the measured TA value at 3.44 eV and time zero.

Thus with Eq. (3),

$$I_T = I_0\left(\frac{1}{10^{A_{2.35eV}}} - kA_{LU}\right)$$

and with Eq. (4),

$$A_{HO^*} = log_{10}(\frac{I_0}{I_T}) = -log_{10}(\frac{1}{10^{A_{2.35eV}}} - kA_{LU}) \tag{6}$$

The constant k in Eq. (6) contains the coefficient of the stimulated emission intensity of the excited state electrons. The HO* curves are calculated before normalization and are then normalized such that the total electrons in YOYO-1 are within (-)1 to (+)1 near the beginning of the delay time, and approach zero at longer time because permanent ionization of YOYO-1 is rare under our experimental conditions, beyond the detection of the TA's signal to noise level. A more accurate normalization factor can be established in the future if the absorption cross-section of the hot-ground-state electrons is measured. An example of this data treatment has been shown in the supporting information **Fig. S5**. This data treatment helps to visualize the hot-ground-state absorption that has been saturated by the strong SE signal of YOYO-1.

The decay lifetimes of molecules at excited and ground state are fitted with a multi-exponential function convoluted with the instrument response function (IRF). The results are shown in Table 1]. The shorter

Table 1
Excited $|LU^1>$ electron decay (e) and $|HO^1>$ refill lifetimes of YOYO-1 in.(A) water, (B) DMSO, and (C) DNA solution.

		Pre-exponential factor (%)				Lifetimes (ps)			
		A_1	A_2	A_3	A_4	τ_1	τ_2	τ_3	τ_4 (ns)
(A)	**LU**	60(2)	23(3)	13(1)	4(1)	2.3(0.1)	33(2)	146(29)	1.2(0.2)
	HO		−55(1)	−45(5)	−11(2)		26(4)	143(12)	1.5(0.1)
(B)	**LU**	42(5)	45(3)	9(2)	4(1)	0.7(0.5)	6.8(1)	29(2)	0.5(0.1)
	HO			−82(1)	−18(1)			22(1)	2.1(0.3)
(C)	**LU**	21(2)		42(2)	37(3)	2(1)		390(20)	6.2(0.8)
	HO	−13(2)		−43(3)	−44(2)	4(1)		410(40)	8.2(1.2)

Note. See supporting information **Fig. S6** for an example fitting of each. (Error) represents the standard deviation of two different samples and multiple fittings. All fittings have $R^2 > 0.98$.

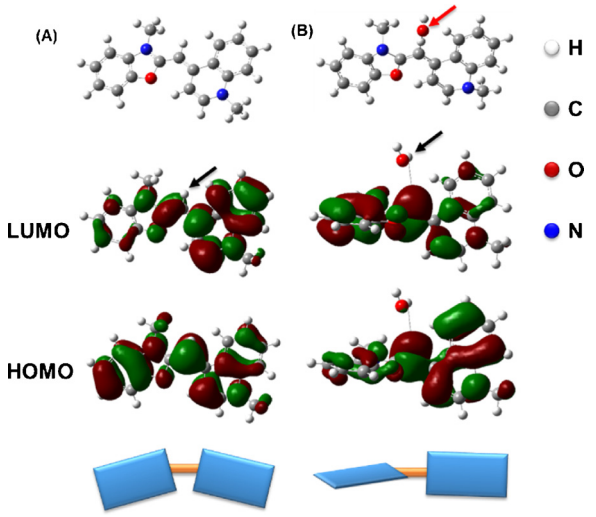

Fig. 7. The density functional theory (DFT)-calculated HOMO and LUMO electron clouds, and the most stable geometry of the methine group for (A) YO and (B) YO with an OH^- near the methine group. The red arrow indicates the chemical difference between the two, black arrows highlight the methine hydrogen, and the green and red balloons represent the electron clouds.

lifetimes are consistent with water hydrogen bond reformation time (~1–2 ps) [56,58–60], the average (sum($A\tau$)/sum(A), where A is the preexponential factor and τ is the lifetime) of the two lifetimes 33 ps and 146 ps is 74 ps, which is consistent with free YOYO-1 rotation in water ~60 ps reported in the literature [17]; DMSO dye coupling ~7 ps [61], DMSO wobbling lifetime ~20 ps [59]; and a lifetime at ~400 ps is observed in DNA which is consistent with the conformational change of water bound to DNA molecules ~450 ps [62]. The longer lifetimes at a few to several nanoseconds are consistent with YOYO-1's long-lived fluorescent decay lifetimes [17].

DFT calculations were performed to compare the molecular structures when the hydrogen at the methine group is pulled away from YOYO-1. The YO molecule favors a planar structure as expected (Fig. 7A). The electron density at the hydrogen at the methine group contributes to the HOMO while it does not contribute to the LUMO (left the black arrow in Fig. 7), making it vulnerable at the excited state. For example, when an OH^- (O_2 should do the same thing too) is placed near the hydrogen of the methine group, it pulls the hydrogen away from the methine (Fig. 7B). The rest of the molecule adapts a perpendicular geometry between the two moieties connected by the bridging methine, with uneven distributions of electron densities.

4. Discussion

The fluorescence results of YOYO-1 on the glass slides suggest a mechanism other than the intramolecular rotation and the energy transfer mechanism. It is reasonable to assume that the immobilization has a certain degree of effect on the free rotation of the molecules. Thus, a larger quantum yield should have been observed for YOYO-1 in water yet the value still approaching zero, the same value observed in the bulk solution. If photo-isomerization, hula-twist [1], or wobbling is responsible for the quenching, the molecule should have remained non-fluorescent when these movements are allowed in all three cases (dye, in water, or in hexane). In order to explain the increased fluorescence in air and hexane, an alternative theory should be considered. Intermolecular charge transfer could explain the results as charge transfer to the solvent should be allowed in the water, but not in hexane or air. One large assumption above is that the physical properties of YOYO-1 molecules themselves are treated roughly equally in each environment. But it is possible that the environmental change affects the YOYO-1 properties. Three important environmental factors are viscosity, polarity, and the degree of intramolecular aggregation. The effect of viscosity supports our results that rotation is hindered because water is ~3 times more viscous than hexane, 8.9×10^{-4} Pa s compared to 3.0×10^{-4} Pa s respectively and the fluorescence is increased in hexane. This is opposite to the trend that rotation should be slower in water than in hexane thus YOYO-1 should have been brighter in water than in hexane if viscosity is the major factor. One original experiment in the literature about the effect of solvent viscosity on dye fluorescence is done by changing the temperature of a dye-glycerol-water or similar solution [26,63]. These experiments cannot exclude the possibility of intermolecular charge transfer because temperature also affects the charge transfer and dye-solvent interaction. Solvent polarity could be another possible explanation because typically, an increase of polarity will cause a lower solvent relaxed excited energy level, leading to a decrease in fluorescence for polar or charged dyes like YOYO-1. YOYO-1 is known to form intramolecular H-aggregates. Less than an order of magnitude change in the fluorescence quantum yield could be explained by intramolecular aggregation if the degree of aggregation is affected by the environment [64].

The TA results also favor an intermolecular charge transfer mechanism better than the intramolecular interaction mechanism. Positive absorption signal of total electrons in YOYO-1 is observed in both water (Fig. 6**A** purple curve) and in DMSO (Fig. 6**B** purple curve). This phenomenon is unlikely to be explained by the intramolecular π electron transfer mechanism proposed in the literature which predicts a flat and zero total absorption [19]. If the excited electron breaks the bridging π bond, positions the molecule in twisted geometry or rotation, or transfers the molecule to a triplet state, or relaxes via a Förster resonance energy transfer process, then, either electron conservation should be observed when all of these electrons still absorb light within our observation window, or a net loss of electrons should be observed if the electron/electrons no longer absorb light in our observation wavelengths. Our observation of electron net gain disfavors these mechanisms. Thus, extra electron donors must be considered. One possible electron donor source is the intermolecular charge transfer (YOYO-1 could gain an electron from or lose a hydrogen cation to the solvent molecules) [8,65–67]. Another source could be an electron from the sigma or non-bonding orbitals of YOYO-1 that does not change the electronic energy structure of the molecule when moved. In both cases, our data suggest that the relaxation of the HOMO vacancy at the hot-ground-state is the first step of relaxation. The source of the electrons are more likely from the solvent rather than from YOYO-1 itself given that solvent-dye charge transfer is a commonly observed phenomenon in photosynthesis systems, where hydrogen bonds are considered effective electron donors [8,33,36,65–71]. The detailed mechanism can be a direct charge flow via hydrogen bond or a two-step Dexter electron transfer observed in many systems [36,72,73]. This hypothesis is supported by the DFT calculations (Fig. 7).

In water and DMSO solutions, the fluorescence quantum yields of YOYO-1 are known to be almost zero, and the excited molecules are known to rotate at the bridging carbon (photo-isomerization). The data observed here perfectly explains both conclusions. Right after the excitation, the positive electron vacancy is neutralized by an electron (lifetime ~2 ps) from outside of the HOMO-LUMO electrons (step 1 in Fig. 6**A, B**), pushing the whole molecule (nuclei) to an upper vibrational state and a free electron in the LUMO. The molecule is negatively ionized to a radical if the electron is from another molecule and a dipole is created if the electron is from an internal sigma-bond electron. This process (a few ps in water) is much faster than the fluorescent relaxation of the excited electron to the ground states (lifetime ~4 ns in DNA) [17], dominating the non-radiative decay pathway and making the fluorescence quantum yield in water and DMSO almost negligible. Then, the free excited electrons transfer out of the system to fill the outside positive charge (step 2 in Fig. 6A, **B**) which quenches the radicals. The injection of an extra electron into the π system changes the C=C double bond to a near single bond condition, and thus enables the

photoisomerization. The quencher cannot be identified in this measurement but is highly suspected to be water/DMSO and/or oxygen that can donate an electron or accept a proton in step 1 (Fig. 6).

The TA data of YOYO-1 in DNA solution suggest that the HOMO relaxation via charge transfer is hindered because no net gain of electrons is observed (Fig. 6C). The fluorescence quantum yield of YOYO-1 in DNA is known to be ~50% [22,24], a high value indicating that the fast charge transfer quenching should have been blocked because the intercalation of YOYO-1 in the DNA basepairs protects the molecule from the solvent charge donor. Thus, S_0* electrons are not observed during the whole excitation and relaxation processes. Dye photophysics is known to be dependent on the binding geometry of YOYO-1 in DNA thus a high DNA:dye ratio is used in this report to minimize the number of non-intercalated dyes [23]. If charge transfer still happens in this situation, its effect spans the long lived excited states and is undetected in our TA measurement. In the literature, intercalated YOYO-1 is known to photo-cleave DNA molecules at relatively high illumination intensities, which means charge transfer must also happen under that condition to generate radicals in the solution.

The decay results in Table 1 suggest that in water and DMSO, about half of the excited molecules, 60%, and 40% respectively, relax via the same solvent molecules that directly bind to the molecules via a fast charge exchange in less than a few picoseconds (Fig. 6). This nonradiative relaxation is independent of the solvent viscosity because it is in the faster time domain than the diffusive solvation dynamics. Giving the fast electron exchange rate, it is likely to be a Dexter energy transfer process [74], consistent with a typical solute-solvent electron transfer dynamics [8,10,13]. The rest of the excited molecules live longer and rotate or move away from the solvent molecule that has donated the charges. Eventually, the negative charge on the dye molecule recombines with the positive charge either on the same solvent molecule or a different solvent molecule depending on the stability of the charges on the molecules. Possibly with the same molecule due to the Coulombic attraction between the positive and the negative charges but only recombine at a binding geometry. This relaxation is dependent on the solvent viscosity. Both decays are nonfluorescent and should be the major physical origin of the nonradiative decay pathways. Very few excited dye molecules survive to illuminate. In DNA, however, ~20% excited molecules nonradiative relaxed at 2–4 ps, ~40% relaxed via the interaction between the dye, the DNA bases, and solvent which can form radicals; and ~40% molecules can survive to give fluorescent signals.

The shape of the ground-state bleaching band (hole absorption) of YOYO-1 in water and DNA does not change much over time but a noticeable change is observed in DMSO (Fig. 4). A possible reason can be that YOYO-1 gets hotter in DMSO than the other two cases. This hypothesis is consistent with the larger amount of hot-ground-state electron calculated from the spectra (Fig. 6B). YOYO-1 aggregation and FRET has been observed but they are unlikely to be the major quenching mechanism because the same phenomena are also observed for diluted monomer YO [20]. The shorter decay lifetimes of ESA than the triplet state lifetime (> 10 μs) [75,76] excludes a significant population of triplet-state YOYO-1, consistent with an estimation of less than 0.1% triplet probability for excited typical cyanine dyes [77].

5. Conclusions

In summary, we have proposed a method for transient absorption spectroscopy to deconvolute the hot-ground-state absorption from the stimulated emission signal and apply it to study the YOYO-1 fluorescence quenching mechanism in polar solvents. After photoexcitation of YOYO-1, we speculate that intermolecular charge transfer quenches the HOMO of the excited molecules in water and DMSO (making $[YOYO\text{-}1]^{-1}$ radical anions), which is responsible for its initial fluorescence quenching. The energy of the excited electron can be relaxed using the existing energy levels of the solvents and no transient energy levels are needed on the dye molecule. The charge transfer process is significantly blocked when YOYO-1 is intercalated in the DNA basepairs or is dried on a glass surface, which greatly increases YOYO-1's fluorescence quantum yield. This experimental observation highly recommends including both electronic and molecular dynamics between the dye molecules and the solvent molecules in the future theoretical calculations for organic dye photophysics. We conclude that the intramolecular rotation is a consequence of intermolecular charge transfer after photoexcitation, rather than the previously believed major nonradiative decay pathway of the excited molecules. This conclusion leads to a dramatically different polymethine dye designing principle: a charge insulating may work to stop the charge transfer, and thus significantly increase the dye's fluorescence quantum yield in polar solvents, while steric hindrance for rotation may not work.

Acknowledgements

The authors thank the National Science Foundation under Grant No. CHE-0947031 for instrumental support; thank the National Institutes of Health Award No. R15HG009972; thank Dr. Michael Jensen and his group for help in UV–vis measurements; thank Dr. Hugh Richardson, Kurt Sy Piecco and Juvinch Vicente for beneficial discussions; thank Ohio University faculty startup program, Nanoscale and Quantum Phenomena Institute (NQPI), and Condensed Matter and Surface Science Program (CMSS) for financial support.

Appendix A. Supplementary data

Supplementary material related to this article can be found, in the online version, at doi:https://doi.org/10.1016/j.jphotochem.2018.09.012.

References

[1] J.R. Lakowicz, Principles of Fluorescence Spectroscopy, 3rd ed., Springer, US, 2006.
[2] B. Dereka, M. Koch, E. Vauthey, Looking at photoinduced charge transfer processes in the IR: answers to several long-standing questions, Acc. Chem. Res. 50 (2017) 426–434.
[3] S. Park, A.L. Fischer, Z. Li, R. Bassi, K.K. Niyogi, G.R. Fleming, Snapshot transient absorption spectroscopy of carotenoid radical cations in high-light-acclimating thylakoid membranes, J. Phys. Chem. Lett. 8 (2017) 5548–5554.
[4] R. Dieter, W. Albert, Kinetics of fluorescence quenching by electron and H-atom transfer, Isr. J. Chem. 8 (1970) 259–271.
[5] J. Zhao, J. Chen, Y. Cui, J. Wang, L. Xia, Y. Dai, P. Song, F. Ma, A questionable excited-state double-proton transfer mechanism for 3-hydroxyisoquinoline, Phys. Chem. Chem. Phys. 17 (2015) 1142–1150.
[6] A.V. Marenich, C.J. Cramer, D.G. Truhlar, Universal solvation model based on solute electron density and on a continuum model of the solvent defined by the bulk dielectric Constant and atomic surface tensions, J. Phys. Chem. B 113 (2009) 6378–6396.
[7] X. Ma, J. Hua, W. Wu, Y. Jin, F. Meng, W. Zhan, H. Tian, A high-efficiency cyanine dye for dye-sensitized solar cells, Tetrahedron 64 (2008) 345–350.
[8] G.-J. Zhao, J.-Y. Liu, L.-C. Zhou, K.-L. Han, Site-selective photoinduced electron transfer from alcoholic solvents to the chromophore facilitated by hydrogen bonding: a new fluorescence quenching mechanism, J. Phys. Chem. B 111 (2007) 8940–8945.
[9] G.-J. Zhao, K.-L. Han, Early time hydrogen-bonding dynamics of photoexcited coumarin 102 in hydrogen-donating solvents: theoretical study, J. Phys. Chem. A 111 (2007) 2469–2474.
[10] Y. Nagasawa, A.P. Yartsev, K. Tominaga, A.E. Johnson, K. Yoshihara, Temperature dependence of ultrafast intermolecular electron transfer faster than solvation process, J. Chem. Phys. 101 (1994) 5717–5726.
[11] W. Rettig, Photoinduced charge separation via twisted intramolecular charge transfer States, Electron Transfer I, Springer, 1994, pp. 253–299.
[12] T. Fonseca, B.M. Ladanyi, Breakdown of linear response for solvation dynamics in methanol, J. Phys. Chem. 95 (1991) 2116–2119.
[13] Y. Nagasawa, A.P. Yartsev, K. Tominaga, P.B. Bisht, A.E. Johnson, K. Yoshihara, Dynamic aspects of ultrafast intermolecular electron transfer faster than solvation process: substituent effects and energy gap dependence, J. Phys. Chem. 99 (1995) 653–662.
[14] H. Pal, Y. Nagasawa, K. Tominaga, K. Yoshihara, Deuterium isotope effect on ultrafast intermolecular electron transfer, J. Phys. Chem. 100 (1996) 11964–11974.
[15] K. Yoshihara, K. Tominaga, Y. Nagasawa, Effects of the solvent dynamics and vibrational motions in electron transfer, Bull. Chem. Soc. Jpn. 68 (1995) 696–712.
[16] F. Momicchioli, I. Baraldi, G. Berthier, Theoretical study of trans-cis

photoisomerism in polymethine cyanines, Chem. Phys. 123 (1988) 103–112.
[17] A. Fürstenberg, M.D. Julliard, T.G. Deligeorgiev, N.I. Gadjev, A.A. Vasilev, E. Vauthey, Ultrafast excited-state dynamics of DNA fluorescent intercalators: new insight into the fluorescence enhancement mechanism, J. Am. Chem. Soc. 128 (2006) 7661–7669.
[18] N. Milanovich, M. Suh, R. Jankowiak, G.J. Small, J.M. Hayes, Binding of TO-PRO-3 and TOTO-3 to DNA: fluorescence and hole-burning studies, J. Phys. Chem. 100 (1996) 9181–9186.
[19] T.L. Netzel, K. Nafisi, M. Zhao, J.R. Lenhard, I. Johnson, Base-content dependence of emission enhancements, quantum yields, and lifetimes for cyanine dyes bound to double-strand DNA: photophysical properties of monomeric and bichromomphoric DNA stains, J. Phys. Chem. 99 (1995) 17936–17947.
[20] C. Carlsson, A. Larsson, M. Jonsson, B. Albinsson, B. Norden, Optical and photophysical properties of the oxazole yellow DNA probes YO and YOYO, J. Phys. Chem. 98 (1994) 10313–10321.
[21] J.R. Pyle, J. Chen, Photobleaching of YOYO-1 in super-resolution single DNA fluorescence imaging, Beilstein J. Nanotechnol. 8 (2017) 2296.
[22] H.S. Rye, S. Yue, D.E. Wemmer, M.A. Quesada, R.P. Haugland, R.A. Mathies, A.N. Glazer, Stable fluorescent complexes of double-stranded DNA with bis-intercalating asymmetric cyanine dyes: properties and applications, Nucleic Acids Res. 20 (1992) 2803–2812.
[23] A. Larsson, C. Carlsson, M. Jonsson, B. Albinsson, Characterization of the binding of the fluorescent dyes YO and YOYO to DNA by polarized light spectroscopy, J. Am. Chem. Soc. 116 (1994) 8459–8465.
[24] R.W. Sabnis, YOYO 1. In Handbook of Fluorescent Dyes and Probes, John Wiley & Sons, Inc, 2015, pp. 421–424.
[25] P. Selvin, Science innovation' 92: the San Francisco sequel, Science 257 (1992) 885–886.
[26] V. Sundström, T. Gillbro, Viscosity dependent radiationless relaxation rate of cyanine dyes. A picosecond laser spectroscopy study, Chem. Phys. 61 (1981) 257–269.
[27] S. Murphy, G.B. Schuster, Electronic relaxation in a series of cyanine dyes: evidence for electronic and steric control of the rotational rate, J. Phys. Chem. 99 (1995) 8516–8518.
[28] E. Åkesson, V. Sundström, T. Gillbro, Isomerization dynamics in solution described by Kramers' theory with a solvent-dependent activation energy, Chem. Phys. 106 (1986) 269–280.
[29] X. Yang, A. Zaitsev, B. Sauerwein, S. Murphy, G.B. Schuster, Penetrated ion pairs: photochemistry of cyanine dyes within organic borates, J. Am. Chem. Soc. 114 (1992) 793–794.
[30] W. Sibbett, J. Taylor, D. Welford, Substituent and environmental effects on the picosecond lifetimes of the polymethine cyanine dyes, IEEE J. Quantum Electron. 17 (1981) 500–509.
[31] A.W. King, L. Wang, J.J. Rack, Excited State dynamics and isomerization in ruthenium sulfoxide complexes, Acc. Chem. Res. 48 (2015) 1115–1122.
[32] R. Berera, R. van Grondelle, J.T.M. Kennis, Ultrafast transient absorption spectroscopy: principles and application to photosynthetic systems, Photosynth. Res. 101 (2009) 105–118.
[33] J.K. McCusker, Femtosecond absorption spectroscopy of transition metal charge-transfer complexes, Acc. Chem. Res. 36 (2003) 876–887.
[34] H. Ohkita, S. Cook, Y. Astuti, W. Duffy, S. Tierney, W. Zhang, M. Heeney, I. McCulloch, J. Nelson, D.D.C. Bradley, et al., Charge carrier formation in polythiophene/fullerene blend films studied by transient absorption spectroscopy, J. Am. Chem. Soc. 130 (2008) 3030–3042.
[35] M. Kaucikas, D. Nürnberg, G. Dorlhiac, A.W. Rutherford, J.J. van Thor, Femtosecond visible transient absorption spectroscopy of chlorophyll F-containing photosystem I, Biophys. J. 112 (2017) 234–249.
[36] S. Henkel, M.C. Misuraca, Y. Ding, M. Guitet, C.A. Hunter, Enhanced chelate cooperativity in polar solvents, J. Am. Chem. Soc. 139 (2017) 6675–6681.
[37] K. Garg, A.W. King, J.J. Rack, One photon yields two isomerizations: large atomic displacements during electronic excited-state dynamics in ruthenium sulfoxide complexes, J. Am. Chem. Soc. 136 (2014) 1856–1863.
[38] L. Wang, I.-S. Tamgho, L.A. Crandall, J.J. Rack, C.J. Ziegler, Ultrafast dynamics of a new class of highly fluorescent boron difluoride dyes, Phys. Chem. Chem. Phys. 17 (2015) 2349–2351.
[39] Spectroscopy Data Analysis Software - Transient Emissionhttp://ultrafastsystems.com/surface-xplorer-data-analysis-software/ (accessed May 9, 2017).
[40] I. Noda, Generalized two-dimensional correlation method applicable to infrared, Raman, and other types of spectroscopy, Appl. Spectrosc. 47 (1993) 1329–1336.
[41] I.H.M. van Stokkum, D.S. Larsen, R. van Grondelle, Global and target analysis of time-resolved spectra, Biochim. Biophys. Acta - Bioenerg. 1657 (2004) 82–104.
[42] M.J. Frisch, G.W. Trucks, H.B. Schlegel, G.E. Scuseria, M.A. Robb, J.R. Cheeseman, G. Scalmani, V. Barone, B. Mennucci, G.A. Petersson, et al., Gaussian 09, Revision D. 01, Gaussian, Inc., Wallingford CT, 2013.
[43] M.P. Andersson, P. Uvdal, New scale factors for harmonic vibrational frequencies using the B3LYP density functional method with the triple-ζ basis set 6-311 + G (d, P), J. Phys. Chem. A 109 (2005) 2937–2941.
[44] J. Chen, A. Bremauntz, L. Kisley, B. Shuang, C.F. Landes, Super-Resolution MbPAINT for optical localization of single-stranded DNA, ACS Appl. Mater. Interfaces 5 (2013) 9338–9343.
[45] B. Shuang, J. Chen, L. Kisley, C.F. Landes, Troika of single particle tracking programing: SNR enhancement, particle identification, and mapping, Phys. Chem. Chem. Phys. 16 (2014) 624–634.
[46] L. Kisley, J. Chen, A.P. Mansur, B. Shuang, K. Kourentzi, M.-V. Poongavanam, W.-H. Chen, S. Dhamane, R.C. Willson, C.F. Landes, Unified superresolution experiments and stochastic theory provide mechanistic insight into protein ion-exchange adsorptive separations, Proc. Natl. Acad. Sci. U.S.A. 111 (2014) 2075–2080.
[47] S.J. Lord, Z. Lu, H. Wang, K.A. Willets, P.J. Schuck, H.D. Lee, S.Y. Nishimura, R.J. Twieg, W.E. Moerner, Photophysical properties of acene DCDHF fluorophores: long-wavelength single-molecule emitters designed for cellular imaging, J. Phys. Chem. A 111 (2007) 8934–8941.
[48] R.R. Birge, Kodak Laser Dyes, Kodak Publ. J J-169, 1987.
[49] I. Noda, Two-dimensional infrared (2D IR) spectroscopy: theory and applications, Appl. Spectrosc. 44 (1990) 550–561.
[50] I. Noda, Determination of two-dimensional correlation spectra using the Hilbert transform, Appl. Spectrosc. 54 (2000) 994–999.
[51] C.-C. Hung, A. Yabushita, T. Kobayashi, P.-F. Chen, K.S. Liang, Ultrafast relaxation dynamics of nitric oxide synthase studied by visible broadband transient absorption spectroscopy, Chem. Phys. Lett. 683 (2017) 619–624.
[52] S. Vdovic, Y. Wang, B. Li, M. Qiu, X. Wang, Q. Guo, A. Xia, Excited state dynamics of β-carotene studied by means of transient absorption spectroscopy and multivariate curve resolution alternating least-squares analysis, Phys. Chem. Chem. Phys. 15 (2013) 20026–20036.
[53] S.W. Hell, J. Wichmann, Breaking the diffraction resolution limit by stimulated emission: stimulated-emission-depletion fluorescence microscopy, Opt. Lett. 19 (1994) 780–782.
[54] G. Haran, K. Wynne, A. Xie, Q. He, M. Chance, R.M. Hochstrasser, Excited State dynamics of bacteriorhodopsin revealed by transient stimulated emission spectra, Chem. Phys. Lett. 261 (1996) 389–395.
[55] K. Wynne, R.M. Hochstrasser, The theory of ultrafast vibrational spectroscopy, Chem. Phys. 193 (1995) 211–236.
[56] D.H. Son, P. Kambhampati, T.W. Kee, P.F. Barbara, Femtosecond multicolor pump – probe study of ultrafast electron transfer of [(NH3)5RuIIINCRuII(CN)5]- in aqueous solution, J. Phys. Chem. A 106 (2002) 4591–4597.
[57] W. Wohlleben, T. Buckup, H. Hashimoto, R.J. Cogdell, J.L. Herek, M. Motzkus, Pump – deplete – probe spectroscopy and the puzzle of carotenoid dark states, J. Phys. Chem. B 108 (2004) 3320–3325.
[58] R. Rey, K.B. Møller, J.T. Hynes, Hydrogen bond dynamics in water and ultrafast infrared spectroscopy, J. Phys. Chem. A 106 (2002) 11993–11996.
[59] D.B. Wong, K.P. Sokolowsky, M.I. El-Barghouthi, E.E. Fenn, C.H. Giammanco, A.L. Sturlaugson, M.D. Fayer, Water dynamics in water/DMSO binary mixtures, J. Phys. Chem. B 116 (2012) 5479–5490.
[60] H. Bian, H. Chen, Q. Zhang, J. Li, X. Wen, W. Zhuang, J. Zheng, Cation effects on rotational dynamics of anions and water molecules in alkali (Li^+, Na^+, K^+, Cs^+) thiocyanate (SCN^-) aqueous solutions, J. Phys. Chem. B 117 (2013) 7972–7984.
[61] J.-Y. Liu, W.-H. Fan, K.-L. Han, W.-Q. Deng, D.-L. Xu, N.-Q. Lou, Ultrafast vibrational and thermal relaxation of dye molecules in solutions, J. Phys. Chem. A 107 (2003) 10857–10861.
[62] S.K. Pal, L. Zhao, A.H. Zewail, Water at DNA surfaces: ultrafast dynamics in minor groove recognition, Proc. Natl. Acad. Sci. U.S.A. 100 (2003) 8113–8118.
[63] G. Oster, Y. Nishijima, Fluorescence and internal rotation: their dependence on viscosity of the medium, J. Am. Chem. Soc. 78 (1956) 1581–1584.
[64] A. Fürstenberg, T.G. Deligeorgiev, N.I. Gadjev, A.A. Vasilev, E. Vauthey, Structure–fluorescence contrast relationship in cyanine DNA intercalators: toward rational dye design, Chem. – A Eur. J. 13 (2007) 8600–8609.
[65] G.-J. Zhao, K.-L. Han, Hydrogen bonding in the electronic excited State, Acc. Chem. Res. 45 (2012) 404–413.
[66] L. Sun, M. Burkitt, M. Tamm, M.K. Raymond, M. Abrahamsson, D. LeGourriérec, Y. Frapart, A. Magnuson, P.H. Kenéz, P. Brandt, Hydrogen-bond promoted intramolecular electron transfer to photogenerated Ru (III): a functional mimic of tyrosinez and histidine 190 in photosystem II, J. Am. Chem. Soc. 121 (1999) 6834–6842.
[67] X. Peng, F. Song, E. Lu, Y. Wang, W. Zhou, J. Fan, Y. Gao, Heptamethine cyanine dyes with a large stokes shift and strong fluorescence: a paradigm for excited-state intramolecular charge transfer, J. Am. Chem. Soc. 127 (2005) 4170–4171.
[68] N.S. Lewis, D.G. Nocera, Powering the planet: chemical challenges in solar energy utilization, Proc. Natl. Acad. Sci. U.S.A. 103 (2006) 15729–15735.
[69] J.M. Zaleski, C.K. Chang, G.E. Leroi, R.I. Cukier, D.G. Nocera, Role of solvent dynamics in the charge recombination of a donor/acceptor pair, J. Am. Chem. Soc. 114 (1992) 3564–3565.
[70] P.B. Petersen, S.T. Roberts, K. Ramasesha, D.G. Nocera, A. Tokmakoff, Ultrafast N – H vibrational dynamics of cyclic doubly hydrogen-bonded homo- and heterodimers, J. Phys. Chem. B 112 (2008) 13167–13171.
[71] A.J. Olaya, P.-F. Brevet, E.A. Smirnov, H.H. Girault, Ultrafast population dynamics of surface-active dyes during electrochemically controlled ion transfer across a liquid|liquid interface, J. Phys. Chem. C 118 (2014) 25027–25031.
[72] G. Ulrich, R. Ziessel, A. Harriman, The chemistry of fluorescent bodipy dyes: versatility unsurpassed, Angew. Chem. Int. Ed. (Engl.) 47 (2008) 1184–1201.
[73] L.B. Picraux, A.L. Smeigh, D. Guo, J.K. McCusker, Intramolecular energy transfer involving Heisenberg spin-coupled dinuclear iron – oxo complexes, Inorg. Chem. 44 (2005) 7846–7859.
[74] D.L. Dexter, A theory of sensitized luminescence in solids, J. Chem. Phys. 21 (1953) 836–850.
[75] M. Shimizu, S. Sasaki, M. Kinjo, Triplet fraction buildup effect of the DNA–YOYO complex studied with fluorescence correlation spectroscopy, Anal. Biochem. 366 (2007) 87–92.
[76] G.B. Strambini, B.A. Kerwin, B.D. Mason, M. Gonnelli, The triplet-state lifetime of indole derivatives in aqueous solution, Photochem. Photobiol. 80 (2007) 462–470.
[77] T. Ha, P. Tinnefeld, Photophysics of fluorescent probes for single-molecule biophysics and super-resolution imaging, Annu. Rev. Phys. Chem. 63 (2012) 595–617.